THE ASTROPHYSICAL JOURNAL, 613:L25–L28, 2004 September 20

PROTON ACCELERATION BEYOND 100 EeV BY AN OBLIQUE SHOCK WAVE IN THE JET OF 3C 273

YASUKO S. HONDA[1] AND MITSURU HONDA[2]

Received 2004 June 2; accepted 2004 August 4; published 2004 August 18

ABSTRACT

We estimate the highest energy of a proton diffusively accelerated by a shock in knot A1 of the jet in luminous nearby quasar 3C 273. Referring to the recent polarization measurements using very long baseline interferometry, we consider the shock propagation across magnetic field lines, namely, configuration of the oblique shock. For larger inclination of the field lines, the effects of particle reflection at the shock front are more pronounced, to significantly increase acceleration efficiency. The quasiperpendicular shock turns out to be needed for safely achieving the proton acceleration to the energy above 100 EeV (10^{20} eV) in a parameter domain reflecting conceivable energy restrictions.

Subject headings: acceleration of particles — galaxies: jets — magnetic fields — methods: numerical — quasars: individual (3C 273) — shock waves

1. INTRODUCTION

The core-dominated quasar 3C 273 is one of the most confirmed objects on account of its high optical luminosity and low redshift ($z = 0.158$; Bridle & Perley 1984). The image obtained with the refurbished *Hubble Space Telescope* (*HST*) revealed that the narrow optical jet consists of discrete knots (Bahcall et al. 1995, hereafter B95) associated with shocks. In radio bands the high linear polarization and featureless spectra imply that the observed emission from the knots is originated in the synchrotron radiation of electrons (and possibly positrons). If the optical emission is also of the synchrotron origin, in situ acceleration of electrons must be just taking place, as they are compatible with the synchrotron lifetime inferred from magnetic field strength (Meisenheimer et al. 1989, hereafter M89). Polarization data in optical bands are similar to those in radio ones and suggest that the optical emission is attributed to the synchrotron losses of accelerated electrons (Röser & Meisenheimer 1991, hereafter RM91; Conway et al. 1993, hereafter C93; Röser et al. 1996). In the brightest knot A, the observed power-law spectrum ($S_\nu \propto \nu^{-\alpha}$) can be fitted by the index of $\alpha = 0.45 \pm 0.10$ (M89), close to the canonical value of $\alpha = (\alpha_e - 1)/2 \sim 0.5$ for the electron spectral index $\alpha_e \sim 2$, expected for Fermi acceleration at strong nonrelativistic shocks.

As far as such an acceleration mechanism works for electrons, the same mechanism will operate for the acceleration of ions, providing that their abundance in the jet is finite (e.g., Rawlings & Saunders 1991). One of the most promising mechanisms is the diffusive shock acceleration (DSA) involving resonant scattering of injected particles, in which the particles trapped in a mean magnetic field are resonantly scattered by the Alfvén waves superposed on the mean field (for a review, see Drury 1983; Blandford & Eichler 1987; Jones & Ellison 1991; Longair 1992, hereafter L92), so as to migrate back and forth between the upstream and downstream region of the shock. As a consequence, the particles are accelerated, receiving energy from the shock. In this context, Biermann & Strittmatter (1987) have discussed the possibility of ultrahigh energy acceleration of protons. However, their description was limited to a simple case for parallel shock propagating along magnetic field lines. Rachen & Biermann (1993) estimated the highest proton energy as $\sim 10^{21}$ eV, but it seems to be rather optimistic.

For precise evaluation of the highest energy, it is important to consider the actual magnetic field geometry in the acceleration site. With regard to this point, a helical pattern of the magnetized jet has recently been observed by the Faraday rotation measures in the *Highly Advanced Laboratory for Communications and Astronomy* VLBI Space Observatory Programme (Asada et al. 2002), and it appears to self-organize a *double helical* structure (Lobanov & Zensus 2001, hereafter LZ01). In such a filamentary jet, expected is that a huge current ($\sim 10^{16}$ A; C93) generates substantial magnetic fields transverse to the filaments (Honda et al. 2000; Honda & Honda 2002, hereafter HH02). Anyhow, when allowing shock propagation along the jet concomitant with *nonparallel* components of the magnetic fields, the shock likely crosses the field lines. This corresponds to the configuration of the "*oblique shock*," for which acceleration efficiency is higher than that for the parallel shock, owing to the effects of mirror-reflection of particles at the shock front (Jokipii 1987; Ostrowski 1988, hereafter O88).

In this Letter, we report a result of the numerical analysis for the highest energy of a proton diffusively accelerated by the oblique shock in knot A1 of the 3C 273 jet. The present model of the oblique DSA is on the basis of the first-order Fermi mechanism including the resonant scattering of particles by the Kolmogorov turbulence. Concerning the quench of acceleration and energy loss processes, a more solid argument is expanded. We demonstrate that for an expected range of radiation energy density, the maximum proton energy exceeding 10^{20} eV is *safely* achieved, especially for quasiperpendicular shock acceleration.

2. THE MODEL OF DIFFUSIVE SHOCK ACCELERATION AT 3C 273/A1

2.1. *Physical Properties of Knot A1*

Below we outline the physical properties and parameters at the knot in the leading edge of the jet of 3C 273, which is specified as "knot A1" (B95) or "knot A" in earlier literatures. The knot A1 is well resolved in optical wavelengths (0.″1 for *HST*), and its radius is about 1 kpc (Röser et al. 2000, hereafter R00). This optical core is encased in the larger radio cocoon whose half-width is ~2 kpc (B95), and the overall structure

[1] Department of Electrical and Information Engineering, Kinki University Technical College, Mie 519-4395, Japan; yasuko@ktc.ac.jp.
[2] Plasma Astrophysics Laboratory, Institute for Global Science, Mie 519-5203, Japan.

seems to correspond to the "hot spot" (in the nomenclature for Fanaroff-Riley II sources; Rachen & Biermann 1993), which may be related to the upper limit of the size of shocks. The key feature of this knot is that X-ray flux is more prominent than that observed in the other knots (Marshall et al. 2001, hereafter M01). Extrapolating the radio-to-optical spectrum to the high-energy region approximately reproduces the observed X-ray continuum (R00). Accordingly, for the X-ray as well, the power-law spectrum (with index $\alpha = 0.60 \pm 0.05$; M01) can be explained by the electron-synchrotron model (Sambruna et al. 2001), rather than the other models invoking the inverse Compton scattering of electrons. The size of the X-ray halo, where a large amount of energetic particles is probably drifting, appears to be larger than that of the radio hot spot (R00; M01), implying that the spatioscale of the confinement region of accelerated particles tends to be larger than that of the shock accelerator.

In the knot distant more than ~20 kpc from core (B95), the flow is decelerated to the weak relativistic speed of $(0.21 \pm 0.04)c$ (M89), where c is the speed of light, although in the vicinity of the core, superluminal motion of ejecta is observed. The flow may be collimated by magnetic fields (HH02), resulting in no significant radial expansion. Polarization measurements suggest the ordered magnetic field, and its strength is of the order of submilligauss at this knot (M89; R00). The degree of polarization increases toward the direction of the bending extended structure, called "inner extension" (RM91), indicating that the field lines are inclined with respect to the jet axis.

2.2. *Particle Acceleration by an Oblique Shock*

For knot A1, presuming the shock speed to be nonrelativistic is adequate for modeling the DSA based on the Fermi-I mechanism (Gaisser 1990, hereafter G90). We consider the fast-mode oblique shock, for which magnetic field strength is boosted to $B_2 = (\cos^2\theta_1 + r^2\sin^2\theta_1)^{1/2} B_1$, where the subscripts $i =$ "1" and "2" indicate the upstream and downstream region, θ_i denotes the inclination angle of the mean magnetic field line with respect to the direction normal to shock surface, and r is the shock compression ratio. In contrast with the case of the parallel shock with $\theta_1 = \theta_2 = 0°$ in which particles are deflected solely because of scattering by magnetic field fluctuations, in the $\theta_1 \neq 0°$ case a fraction of the particles is directly reflected at the shock front by the boosted field in the region 2, conforming to the conservation of the magnetic moment. Expected here is that the effect of this mirror-reflection leads to significant reduction of acceleration time, viz., increase of acceleration efficiency (e.g., Kirk & Heavens 1989, hereafter KH89). Indeed, this effect has been confirmed by the Monte Carlo simulations for a nonrelativistic shock (Naito & Takahara 1995; Ellison et al. 1995).

For calculation of energy gain of particles, we transfer from plasma rest frames of the regions 1 and 2 to a proper frame where the electric field vanishes (de Hoffmann & Teller 1950, hereafter DT50), then transform physical variables back to those in the original frame (O88). The mean acceleration time can be defined as the cycle time for one back-and-forth between regions 1 and 2 divided by the energy gain per encounter with the shock (G90). An improved calculation including the mirror-reflection effects yields the following resultant of the mean acceleration time (Kobayakawa et al. 2002, hereafter K02):

$$t_{a,\,\mathrm{acc}} = \frac{3r_{g,\,a}\beta_a c}{U_1^2}\,\frac{r\eta_a}{r-1}\left\{\cos^2\theta_1 + \frac{\sin^2\theta_1}{1+\eta_a^2} + \frac{r\cos^2\theta_1 + [r^3\sin^2\theta_1/(1+\eta_a^2)]}{(\cos^2\theta_1 + r^2\sin^2\theta_1)^{3/2}}\right\}, \qquad (1)$$

for arbitrary species of particle "a". Here, U_1 is the shock speed, $\beta_a = v_a/c \simeq 1$, and v_a is the speed of the particle, and furthermore, $\eta_a = \ell_{a,\,\parallel}/r_{g,\,a}$, where $\ell_{a,\,\parallel}$ is the mean free path (mfp) along the magnetic field line, $r_{g,\,a} = \beta_a\gamma_a m_a c^2/(|q_a|B_1)$ the gyroradius in the region 1, $\gamma_a = (1-\beta_a^2)^{-1/2}$, and m_a and q_a the rest mass and charge of the particle, respectively. Note the allowable range of the field inclination angle of $\theta_1 \leq \theta_{1,\,\max} = \cos^{-1}(U_1/c)$, where $\theta_{1,\,\max}$ is called the de Hoffmann-Teller (HT) limit for oblique shocks (DT50; KH89; K02).

In equation (1), the shock compression ratio is fixed to $r = 4$ for a strong nonrelativistic shock. We compare the magnetic fluctuations involved in the shock to the Kolmogorov turbulence establishing the spectral intensity of $I(k) \propto k^{-5/3}$, where k is the wavenumber of the Alfvén waves (e.g., Biermann & Strittmatter 1987, hereafter BS87). In the circumstances that when the wave-particle resonance condition, $r_{g,\,a} \sim k^{-1}$, is satisfied, the pitch-angle scattering of particles becomes effective, the mfp can be denoted as $\ell_{a,\,\parallel} \sim [3r_{g,\,a}/(2b)](r_{g,\,\max}/r_{g,\,a})^{2/3}$. Here, $r_{g,\,\max}$ defines the maximum resonant gyroradius, and b (≤ 1) the ratio of turbulent to mean magnetic energy density. Note that setting to $b \sim \mathcal{O}(1)$ makes the local inclination angle fluctuate around the average θ_i. Nevertheless, this choice is feasible, as long as the trajectory of the guiding center drift of the particles bounded by the mean field is not disturbed, that is, the characteristic timescale of the drift in the shock vicinity is shorter than the coherence time for the resonant scattering. As shown later, this condition turns out to be fairly satisfied in the allowable range of $r_{g,\,a} \leq r_{g,\,\max}$. In this aspect, let us set to the critical value, $b = 1$, adequate for simple estimation of the *achievable highest* energy of accelerated particles, and convenient for making a direct comparison with a previous result in the special case for parallel shock [BS87; expecting $3b(U_1/c)^2 \sim 1$].

As the jet seems to be *nonuniformly filled*, having helical filaments (LZ01), we allow the hot spot with its radius R_{HS} to contain *multipartite* shock disks, whose radial size each is associated with the order of maximum turbulent wavelength, $\sim k_{\min}^{-1}$. In order for the resonance to be locked in phase, the gyroradius cannot exceed $\sim k_{\min}^{-1}$, which is limited by R_{HS}. That is, we have the relation of $r_{g,\,a} \leq r_{g,\,\max} \sim k_{\min}^{-1} \lesssim R_{\mathrm{HS}}$. In a specific case that the knot feature is identified with a *single* shock, we reproduce $k_{\min}^{-1} \sim R_{\mathrm{HS}}$, i.e., $r_{g,\,\max} \sim R_{\mathrm{HS}}$, referred to as the Hillas criterion (Hillas 1984, hereafter H84). Below we regard, in equation (1), $r_{g,\,\max}$ as a variable in the range of $\lesssim R_{\mathrm{HS}}$.

2.3. *The Energy Constraints*

By equating the mean acceleration time (eq. [1]) with the shortest timescale for the most severe energy restriction, we can derive the maximum possible energy of particles, defined

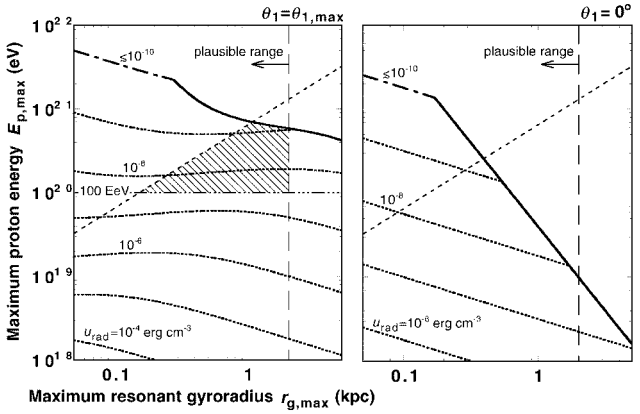

FIG. 1.—Maximum possible energy of accelerated proton $E_{p,\max}$ vs. the maximum resonant gyroradius $r_{g,\max}$ for the inclination angles of magnetic field lines, $\theta_1 = \theta_{1,\max} = 75.^{\circ}5$ (*left*) and $\theta_1 = 0°$ (*right*). The figures have the same axes. The solutions of eq. (2) are plotted for the balance of the mean acceleration time, $t_{p,\mathrm{acc}}$, with the loss timescales for escape ($t_{p,\mathrm{esc}}$; *solid line*), synchrotron ($t_{p,\mathrm{syn}}$; *dot-dashed line*), and photopionization ($t_{p\gamma}$; *dotted lines*). For $t_{p,\mathrm{acc}} = t_{p\gamma}$, the lines are displayed each factor 10 for radiation energy density, u_{rad}, in units of ergs cm^{-3}. Note that those plots for $u_{\mathrm{rad}} \lesssim 10^{-10}$ ergs cm^{-3} overlap the dot-dashed curve. In the left panel, the hatched domain indicates the window where $E_{p,\max}$ exceeds the threshold value of 10^{20} eV (*triple dot-dashed line*) for the conditions of $r_{g,p} \le r_{g,\max}$ (*bottom side of short-dashed line*) and $r_{g,\max} \lesssim 2$ kpc (*left side of long-dashed line*).

as $E_{a,\max} = \gamma_a m_a c^2$. For the proton ($a =$ "p"), the time-balance equation can be expressed as

$$t_{p,\mathrm{acc}}(\gamma_p, \theta_1, r_{g,\max}) = \min\,[t_{p,\mathrm{syn}}(\gamma_p), t_{p\gamma}(\gamma_p, u_{\mathrm{rad}}), t_{p,\mathrm{esc}}(\gamma_p, r_{g,\max}), t_{\mathrm{sh}}]. \quad (2)$$

Here, $t_{p,\mathrm{syn}} \simeq 6\pi m_p^3 c/(\sigma_{\mathrm{T}} m_e^2 \gamma_p B_1^2)$ defines the cooling time for synchrotron radiation by the accelerated protons (L92), where σ_{T} is the Thomson cross section. The loss timescale may be rewritten as $t_{p,\mathrm{syn}} \sim 1 \times 10^{14}(10^{11}/\gamma_p)(0.7\ \mathrm{mG}/B_1)^2$ s. Also, the inelastic collision with photons involving photopionization can be a competitive energy loss process. For the present purpose, we employ an approximate expression of the loss timescale, $t_{p\gamma} \sim (t_{p,\mathrm{syn}}/200)[B_1^2/(8\pi u_{\mathrm{rad}})]$ (for 3C 273; BS87), where u_{rad} stands for average energy density of target radiation fields. The above expression scales as $t_{p\gamma} \sim 1 \times 10^{12}(10^{11}/\gamma_p)(10^{-8}\ \mathrm{ergs\ cm^{-3}}/u_{\mathrm{rad}})$ s. In addition to the loss due to such elementary processes, the particle escape itself quenches the acceleration. The escape time can be estimated as $t_{p,\mathrm{esc}} \simeq 1.5R_{\mathrm{XH}}^2/[c\ell_{p,\|}(\gamma_p, r_{g,\max})]$ (H84), where R_{XH} ($\gtrsim R_{\mathrm{HS}}$) represents the radius of the X-ray halo confining energetic particles (see § 2.1). The timescale can be expressed as $t_{p,\mathrm{esc}} \sim 8 \times 10^{11}(R_{\mathrm{XH}}/\ell_{p,\|})(R_{\mathrm{XH}}/5\ \mathrm{kpc})$ s. Furthermore, the propagation time of the shock through the jet possibly limits the acceleration, while the radial adiabatic expansion is *less* effective for the self-collimating jet (HH02), in contrast with spherically expanding supernova remnant shocks (K02). The shock propagation time t_{sh} may be interpreted as the age of the knot, which is crudely estimated as $\sim L/U_{\mathrm{prop}}$, where L represents a distance from the core to the knot and $U_{\mathrm{prop}}(\sim U_1)$ the speed of proper motion of the knot, to give the scaling of $t_{\mathrm{sh}} \sim 8 \times 10^{12}(L/20\ \mathrm{kpc})(0.25c/U_1)$ s.

3. NUMERICAL SOLUTIONS: THE ACHIEVABLE HIGHEST ENERGY OF ACCELERATED PROTONS

Now, given θ_1, $r_{g,\max}$, and u_{rad}, we self-consistently solve equation (2) for γ_p. Along the explanations mentioned above, at the moment we choose the physical parameters of 3C 273/A1 as $U_1 = 0.25c$ (M89), $B_1 = 700\ \mu$G (R00), $R_{\mathrm{HS}} = 2$ kpc (B95), $R_{\mathrm{XH}} = 5$ kpc (M01), and $L = 20$ kpc (B95). It is noted that the maximum inclination angle of the magnetic field lines reaches $\theta_{1,\max} = \cos^{-1}(U_1/c) = 75.^{\circ}5$ and $\theta_{2,\max} = \tan^{-1}(r\tan\theta_{1,\max}) = 86.^{\circ}3$ for $r = 4$, appropriate for referring to as "quasiperpendicular shock."

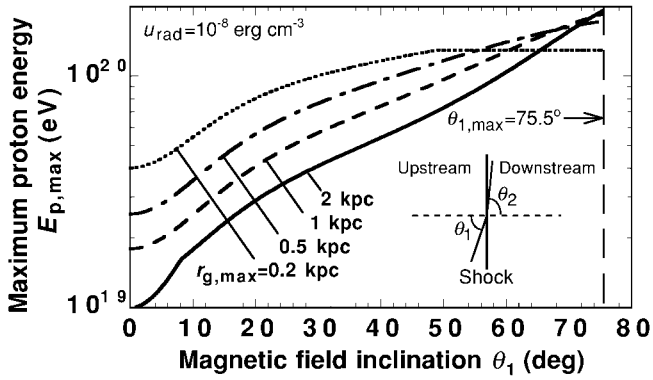

FIG. 2.—Dependence of the maximum proton energy $E_{p,\max}$ on the inclination angle θ_1 for the parameters of $r_{g,\max} = 0.2$ (*dotted line*), 0.5 (*dot-dashed line*), 1 (*dashed line*), and 2 kpc (*solid line*). Here, we have set to $u_{\mathrm{rad}} = 10^{-8}$ ergs cm^{-3}. In the inset, the inclination angles θ_i are limited by the maximum values of $\theta_{1,\max} = 75.^{\circ}5$ for the shock speed of $0.25c$ and $\theta_{2,\max} = 86.^{\circ}3$ for the shock compression ratio 4.

In Figure 1 for $\theta_1 = \theta_{1,\max}$ (*left*) and 0° (*right*), we show $E_{p,\max} = \gamma_p m_p c^2$ as a function of $r_{g,\max}$ ($\sim k_{\min}^{-1}$), for some given values of u_{rad} as a parameter. In a wide range of smaller $r_{g,\max}$ and larger u_{rad}, $E_{p,\max}$ is determined by the balance of $t_{p,\mathrm{acc}} = t_{p\gamma} \propto u_{\mathrm{rad}}^{-1}$ in equation (2) (*dotted lines*). For much smaller u_{rad}, $E_{p,\max}$ saturates, being determined by $t_{p,\mathrm{acc}} = t_{p,\mathrm{esc}} \propto r_{g,\max}^{-2/3}$ in a large $r_{g,\max}$ region (*solid line*), whereas in a small $r_{g,\max}$ region, by $t_{p,\mathrm{acc}} = t_{p,\mathrm{syn}}$ for $u_{\mathrm{rad}} \lesssim 10^{-10}$ ergs cm^{-3} (*dot-dashed line*). Even for the chosen (rather small) value of L, t_{sh} cannot be the shortest timescale in the right-hand side of equation (2). In both panels, the bottom side of the short-dashed line is $r_{g,p} \le r_{g,\max}$ and the left side of the long-dashed line is $r_{g,\max} \lesssim R_{\mathrm{HS}} = 2$ kpc, indicating the allowable and plausible region, respectively. Note that a point of intersection of these two lines, which represents the Hillas criterion, $r_{g,p} = r_{g,\max} = R_{\mathrm{HS}}$, is in a marginal region above the solid line. The region of $r_{g,p} \gg r_{g,\max}$ far above the short-dashed line, i.e., $\eta_p^2 \ll 1$ for $b = 1$, can be compared to the "diffusive limit" (O88) that violates equation (1).

In the case of $\theta_1 = 0°$, the values of $E_{p,\max}$ monotonically decrease as $r_{g,\max}$ increases, to exhibit the scaling of $E_{p,\max} \propto r_{g,\max}^{-1/2}$ for the cases of $t_{p,\mathrm{acc}} = t_{p\gamma}$ and $t_{p,\mathrm{acc}} = t_{p,\mathrm{syn}}$, and $E_{p,\max} \propto r_{g,\max}^{-2}$ for $t_{p,\mathrm{acc}} = t_{p,\mathrm{esc}}$. These tendencies reflect the resonant scattering theory in which a longer coherence time (i.e., longer gyroperiod) leads to lower acceleration efficiency. For $\theta_1 \neq 0°$, however, $E_{p,\max}$ is found to be significantly enhanced. As seen in the case of $\theta_1 = \theta_{1,\max}$, the resulting boost of $E_{p,\max}$ is prominent in the region below the short-dashed line. This property suggests a picture that the larger value of $\eta_p \propto (r_{g,\max}/r_{g,p})^{2/3}$ in equation (1) effectively represents larger anisotropy of diffusion coefficients, i.e., for $\eta_p^2 \gg 1$ (corresponding to the "free crossing limit"; O88), $\kappa_{\|} \gg \kappa_{\perp}$, where the subscripts refer to the direction of the magnetic field line; they largely assist the mirror-reflection of particles (see also Fig. 2).

We are particularly concerned with the *actual* maximum energy of the accelerated proton exceeding 10^{20} eV. In the left

panel of Figure 1, the hatched domain indicates the window where $E_{p,\max}$ exceeds 10^{20} eV for the condition of $r_g \leq r_{g,\max} \lesssim 2$ kpc. In this domain, it is found that $E_{p,\max}$ depends largely on the value of $u_{\rm rad}$, which involves a large uncertainty responsible for observation. At this juncture, we infer the value of $u_{\rm rad}$ from comparing the observed highest frequency of radiation with the synchrotron cutoff frequency deduced from the calculated maximum energy of the electron. This is feasible because the X-ray from knot A1 is arguably ascribed to the simple synchrotron emission due to accelerated electrons (§ 2.1). For an electron (a = 'e') the method to obtain the maximum possible energy is analogous to that explained in § 2.3: the time-balance equation can be expressed as $t_{e,\rm acc}(\gamma_e, \theta_1, r_{g,\max}) = \min\,[t_{e,\rm syn}(\gamma_e), t_{\rm ic}(\gamma_e, u_{\rm rad})]$. Here, $t_{e,\rm syn}$ denotes the familiar electron synchrotron timescale, and $t_{\rm ic} = 3m_e c/(4\sigma_{\rm KN}\gamma_e u_{\rm rad})$ the timescale for the inverse Compton scattering (BS87; L92), where $\sigma_{\rm KN}$ is the Klein-Nishina cross section. For $\theta_1 = \theta_{1,\max}$, we have numerically calculated at $E_{e,\max} = \gamma_e m_e c^2$, and the synchrotron cutoff frequency by using the expression of $\nu_c \sim (3/16)(e/m_e^3 c^5)E_{e,\max}^2 B_1$ (BS87). As a consequence, consistency of the calculated ν_c with the observed result $\nu_{c,\rm obs} \gtrsim 10^{17}$ Hz (R00) is found to require $u_{\rm rad} \lesssim 10^{-8}$ ergs cm^{-3} in the region of $r_{g,\max} \lesssim 2$ kpc (not shown in the figure). Note that the upper limit of $u_{\rm rad}$ is close to the value inferred from the energy equipartition, $u_{\rm rad} = B_1^2/(8\pi) \simeq 2 \times 10^{-8}$ ergs cm^{-3}. On the other hand, for $\theta_1 = 0°$ we get $\nu_c \gtrsim 10^{14}$ Hz (BS87) in the same region of $r_{g,\max}$, such that $\nu_c \ll \nu_{c,\rm obs}$.

For the expected value of $u_{\rm rad} \sim 10^{-8}$ ergs cm^{-3}, we see in Figure 1 that at $r_{g,\max} = 2$ kpc, the actual maximum energies of the proton are $E_{p,\max} \sim 2 \times 10^{20}$ eV and 1×10^{19} eV for $\theta_1 = \theta_{1,\max}$ and 0°, respectively. For the $\theta_1 = \theta_{1,\max}$ case, $E_{p,\max}$ always exceeds the threshold of 10^{20} eV in the hatched domain, taking the value of about 2×10^{20} eV, whereas for $\theta_1 = 0°$, $E_{p,\max}$ cannot exceed the threshold, even though taking the peak value of about 6×10^{19} eV at $r_{g,\max} \approx 90$ pc. It is also remarked that in a possible range of $u_{\rm rad} \lesssim 10^{-9}$ ergs cm^{-3}, $E_{p,\max} \gtrsim 5 \times 10^{20}$ eV can be achieved for $\theta_1 = \theta_{1,\max}$.

In Figure 2 for $u_{\rm rad} = 10^{-8}$ ergs cm^{-3}, the θ_1-dependence of $E_{p,\max}$ is shown for some given $r_{g,\max}$ as a parameter. For $r_{g,\max} = 0.5$ and 1 kpc, in the whole range of θ_1, $E_{p,\max}$ are determined by the balance of $t_{p,\rm acc} = t_{p\gamma}$, to take their maximum values at the HT limit, $\theta_1 = \theta_{1,\max}$. For a larger $r_{g,\max} = 2$ kpc and smaller 0.2 kpc, this time-balance also governs in a major range of θ_1, except for the regions of $\theta_1 \lesssim 8°$ and $\gtrsim 49°$, where $E_{p,\max}$ are determined by $t_{p,\rm acc} = t_{\rm esc}$ and limited by $r_{g,p} \leq r_{g,\max}$ giving a constant maximum, respectively. Evidently, we find that the values of $E_{p,\max}$, which are, at $\theta_1 = 0°$, below the threshold of 10^{20} eV, exceed the threshold in the large θ_1 region. For the larger $r_{g,\max}$, $E_{p,\max}$ appears to be more enhanced for variation of θ_1 from 0° to $\theta_{1,\max}$.

4. CONCLUSIONS

Referring to the VLBI observations of helical filaments in the jet of 3C 273, we have estimated the maximum possible energy of protons diffusively accelerated by an oblique shock at knot A1. The hot spot–like feature is regarded as multipartite shock disks or to contain a single shock whose radial size can be smaller than the hot spot radius. The complementary calculation of maximum electron energy ($E_{e,\max}/m_e c^2 \gtrsim 10^7$) suggests that the upper limit of radiation energy density is of the order of $u_{\rm rad} \sim 10^{-8}$ ergs cm^{-3}. We conclude that for a possible $u_{\rm rad}$ range, protons can be accelerated beyond 10^{20} eV safely by the quasiperpendicular shock. The present method might be applicable for solving the problem of in situ acceleration of particles in the other objects, although this work ignores the effects of particle transport, which may be important for making a comparison with results of precedent (Takeda et al. 2003; Abbasi et al. 2004) and future experiments (at the Pierre Auger Observatory, the *Extreme Universe Space Observatory*, and so forth).

REFERENCES

Abbasi, R. U., et al. 2004, Phys. Rev. Lett., 92, 151101
Asada, K., Inoue, M., Uchida, Y., Kameno, S., Fujisawa, K., Iguchi, S., & Mutoh, M. 2002, PASJ, 54, L39
Bahcall, J. N., Kirhakos, S., Schneider, D. P., Davis, R. J., Muxlow, T. W. B., Garrington, S. T., Conway, R. G., & Unwin, S. C. 1995, ApJ, 452, L91 (B95)
Biermann, P. L., & Strittmatter, P. A. 1987, ApJ, 322, 643 (BS87)
Blandford, R., & Eichler, D. 1987, Phys. Rep., 154, 1
Bridle, A. H., & Perley, R. A. 1984, ARA&A, 22, 319
Conway, R. G., Garrington, S. T., Perley, R. A., & Biretta, J. A. 1993, A&A, 267, 347 (C93)
de Hoffmann, F., & Teller, E. 1950, Phys. Rev., 80, 692 (DT50)
Drury, L. O'C. 1983, Rep. Prog. Phys., 46, 973
Ellison, D. C., Baring, M. G., & Jones, F. C. 1995, ApJ, 453, 873
Gaisser, T. K. 1990, Cosmic Rays and Particle Physics (Cambridge: Cambridge Univ. Press) (G90)
Hillas, A. M. 1984, ARA&A, 22, 425 (H84)
Honda, M., & Honda, Y. S. 2002, ApJ, 569, L39 (HH02)
Honda, M., Meyer-ter-Vehn, J., & Pukhov, A. 2000, Phys. Plasmas, 7, 1302
Jokipii, J. R. 1987, ApJ, 313, 842
Jones, F. C., & Ellison, D. C. 1991, Space Sci. Rev., 58, 259
Kirk, J. G., & Heavens, A. F. 1989, MNRAS, 239, 995 (KH89)
Kobayakawa, K., Honda, Y. S., & Samura, T. 2002, Phys. Rev. D, 66, 083004 (K02)
Lobanov, A. P., & Zensus, J. A. 2001, Science, 294, 128 (LZ01)
Longair, M. S. 1992, High Energy Astrophysics, Vol. 1 (Cambridge: Cambridge Univ. Press) (L92)
Marshall, H. L., et al. 2001, ApJ, 549, L167 (M01)
Meisenheimer, K., Röser, H.-J., Hiltner, P. R., Yates, M. G., Longair, M. S., Chini, R., & Perley, R. A. 1989, A&A, 219, 63 (M89)
Naito, T., & Takahara, F. 1995, MNRAS, 275, 1077
Ostrowski, M. 1988, MNRAS, 233, 257 (O88)
Rachen, J. P., & Biermann, P. L. 1993, A&A, 272, 161
Rawlings, S., & Saunders, R. 1991, Nature, 349, 138
Röser, H.-J., Conway, R. G., & Meisenheimer, K. 1996, A&A, 314, 414
Röser, H.-J., & Meisenheimer, K. 1991, A&A, 252, 458 (RM91)
Röser, H.-J., Meisenheimer, K., Neumann, M., Conway, R. G., & Perley, R. A. 2000, A&A, 360, 99 (R00)
Sambruna, R. M., Urry, C. M., Tavecchio, F., Maraschi, L., Scarpa, R., Chartas, G., & Muxlow, T. 2001, ApJ, 549, L161
Takeda, M., et al. 2003, Astropart. Phys., 19, 447